Histol Histopath (1991) 6: 43-53

Histology and Histopathology

Ultrastructural changes in the gracile nucleus of the spontaneously diabetic BB rat

S.S.W. Tay and W.C. Wong
Department of Anatomy, Faculty of Medicine, National University of Singapore, Singapore

Summary. The present study describes the structural changes in the gracile nucleus of the spontaneously diabetic BB rat. At 3-7 days post-diabetes, axons, axon terminals and dendrites showed electron-dense degeneration. Degenerating axons were characterized by swollen mitochondria, vacuolation, accumulation of glycogen granules, tubulovesicular elements, neurofilaments and dense lamellar bodies. Degenerating axon terminals consisted of an electron-dense cytoplasm containing swollen mitochondria, vacuoles and clustering of synaptic vesicles. These axon terminals made synaptic contacts with cell somata, dendrites and other axon terminals. Degenerating dendrites were postsynaptic to normal as well as degenerating axon terminals. At 1-3 months post-diabetes, degenerating electron-dense axons, axon terminals and dendrites were widely scattered in the neuropil. Macrophages containing degenerating electron-dense debris were also present. At 6 months post-diabetes, the freshly degenerating neuronal elements encountered were similar to those observed at 3-7 days. However, there were more degenerating profiles at 6 months post-diabetes compared to the earlier time intervals. Terminally degenerating axons were vacuolated and their axoplasm appeared amorphous. It is concluded that degenerative changes occur in the gracile nucleus of the spontaneously diabetic BB rat.

Key words: Gracile nucleus, BB rat, Diabetes mellitus

Introduction

The spontaneously diabetic «BB» rat was discovered in 1974 by Drs. Reginald and Clifford Chappel at the Bio Breeding Laboratories (Ottawa, Canada). Since its discovery, metabolic and morphologic changes in the islets of Langerhans in the pancreas have been reported (Nakhooda et al., 1977, 1978; Marliss et al., 1982). Proximal motor neuropathy involving the ventral spinal roots has been described in the spontaneously diabetic BB rat (Sima and Thibert, 1982). Peripheral autonomic neuropathy has also been described in both the parasympathetic and sympathetic nerves (Yagihashi and Sima, 1985a,b, 1986a,b). Recently, Sima and Yagihashi (1986) showed ultrastructural changes in the central sensory nerve fibres of the gracile tract in the same species of animal. Ultrastructural findings included an early-occurring malorientation of the axoplasmic neurofilaments, axonal sequestration by honeycombing, and ensuing progressive axonal atrophy. However, as information on the ultrastructural changes in the gracile nucleus of the spontaneously diabetic BB rat is lacking, the present study was undertaken. A brief account of this work has been reported previously (Tay et al., 1988).

Offprint requests to: Dr. S.S.W. Tay, Department of Anatomy, National University of Singapore, 10 Kent Ridge Crescent, Singapore 0511, Singapore

Materials and methods

Animals

Prediabetic male BB rats were obtained from Health Protection branch, Health and Welfare Canada, Ottawa, Ontario (courtesy of Dr. P. Thibert). All animals were placed in individual cages and given rat chow and water *ad libitum*. Urine volume and urine glucose were monitored daily. Onset of diabetes was determined at blood glucose concentration of 400 mg/dL or more. Diabetic rats developed diabetes at mean age of 92 ± 8 days and were subsequently treated daily with a small dose (0.5 - 3.0 U) of protamine zinc insulin. These animals were maintained at fasting hyperglycaemic levels between 300 and 350 mg/dL throughout the period of study. Blood glucose levels were determined on tail vein blood using Glucostix and an Ames glucometer II (Miles Laboratories, Elkhart, Indiana). Groups of 4 diabetic rats were killed by perfusion at 3 and 7 days, and 1,

3 and 6 months post-diabetes. Age- and sex-matched non-diabetes-prone Wistar rats served as controls. Control animals showed fasting blood-sugar levels ranging from 80-120 mg/dL.

Electron Microscopic techniques

At time of killing, each animal was anaesthetized with sodium pentobarbital (50 mg/kg body wt) and perfused with 300 ml of fixative (3% glutaraldehyde and 2% paraformaldehyde) in 0.1M cacodylate buffer (pH 7.4). The brain stem was carefully dissected out and immersed in a fresh solution of fixative and kept at 4° C overnight. The next morning, the area containing the gracile nucleus was trimmed under a stereo-microscope. Thin slices containing the gracile nucleus were placed in ice cold 0.1M cacodylate buffer (pH 7.4) containing 5% sucrose. After two changes of buffer at intervals of 10 min, the tissue slices were post-fixed in 1% osmium tetroxide (containing 1.5% potassium ferrocyanide) for 2 h at 4° C. The tissue blocks were dehydrated in an ascending series of ethanol and then embedded in Araldite.

Semithin sections (1 μm thick) were cut on a Reichert OMU4 ultramicrotome and stained with 1% methylene blue. Selected areas were trimmed for ultrathin sections, which were stained in uranyl acetate and lead citrate and examined in Philips 400T and JEOL 1200 CX electron microscopes.

Results

Control animals

The neurons of the gracile nucleus showed variations in granularity of the Nissl bodies, and in size and shape of the cell body. On closer examination, two types of neurons (based on size and shape) could be distinguished: the preponderant medium-sized neurons, which had an average size of 22 x 15 μm, and the small neurons, which had an average size of 12 x 8 μm. The medium sized neurons had a round or oval nucleus containing a conspicuous nucleolus (Fig. 1). The cytoplasm displayed well-developed paranuclear Golgi apparatus, widely distributed cisternae of rough endoplasmic reticulum and a variable number of lipofuscin granules (Fig. 1). The dendrites generally had a smooth outline identifiable for their pale cytoplasm with neurotubules, profiles of endoplasmic reticulum and mitochondria. The small neurons had a smoother contour and a deeply infolded nucleus (Fig. 2). The scanty cytoplasm contained a small Golgi apparatus, isolated profiles of rough endoplasmic reticulum and a few lipofuscin granules. The neuropil of the gracile nucleus showed wide variations in the diameters of the axons, axon terminals and dendrites (Figs. 1, 2). Axon terminals established synapses with the neuronal somata, the dendrites as well as the axon terminals. Synaptic glomeruli were also commonly encountered. Interspersed amongst the neuronal profiles, there were also numerous glial cells with their characteristic clumping of chromatin materials in their nuclei.

3 days post-diabetes

As early as 3 days post-diabetes, numerous axons, axon terminals and dendrites showed electron-dense degeneration. Degenerating axon terminals were characterized by an electron-dense cytoplasm containing swollen mitochondria and clustering of synaptic vesicles (Figs. 3, 4). Very often, degenerating axon terminals lay in close apposition to cell somata (Fig. 3) or dendrites (Figs. 4, 5). Degenerating axons are present in both myelinated and unmyelinated profiles. These degenerating profiles were identified by the presence of swollen mitochondria, vacuolations, accumulation of glycogen granules, tubulovesicular elements, neurofilaments and dense lamellar bodies (Fig. 6). Degenerating dendrites were characterized by an electron-dense cytoplasm containing cisternae of endoplasmic reticulum and mitochondria; most of these profiles were postsynaptic to normal as well as degenerating axon terminals.

7 days post-diabetes

At this stage, numerous degenerating electron-dense axon terminals were encountered in the neuropil of the gracile nucleus. Each degenerating axon terminal was identified by its small agranular synaptic vesicles and swollen mitochondria in an electron-dense cytoplasm (Figs. 7, 8). Most of these degenerating axon terminals were still in synaptic contacts with dendrites (Fig. 7) or other axon terminals. Myelinated axons showed both electron-dense as well as electron-lucent forms of degeneration (Fig. 9). Degenerating electron-dense myelinated axons usually showed an electron-dense core in the process of being detached from the myelin sheath, and an accumulation of mitochondria. Some swollen myelinated axons showed an amorphous cytoplasm with unidentifiable remnants (Fig. 10). Unaffected axons and axon terminals were randomly distributed amongst the affected degenerating profiles.

1 month post-diabetes

Swollen axon terminals (characterized by accumulation of mitochondria and small agranular synaptic vesicles) were commonly seen at this stage (Fig. 11). Most of the affected axon terminals appeared to be unusually enlarged, containing the characteristic organelles that identified them specifically. Several degenerating myelinated and unmyelinated axons were scattered amongst the degenerating axon terminals and dendrites. Macrophages started to infiltrate into the neuropil and were usually found near the degenerating profiles. Each macrophage was characterized by a large irregular nucleus, with randomly dispersed chromatin materials (Fig. 12). In most of the macrophages seen at this stage, a lot of electron-dense debris was found in

Gracile nucleus of diabetic BB rat

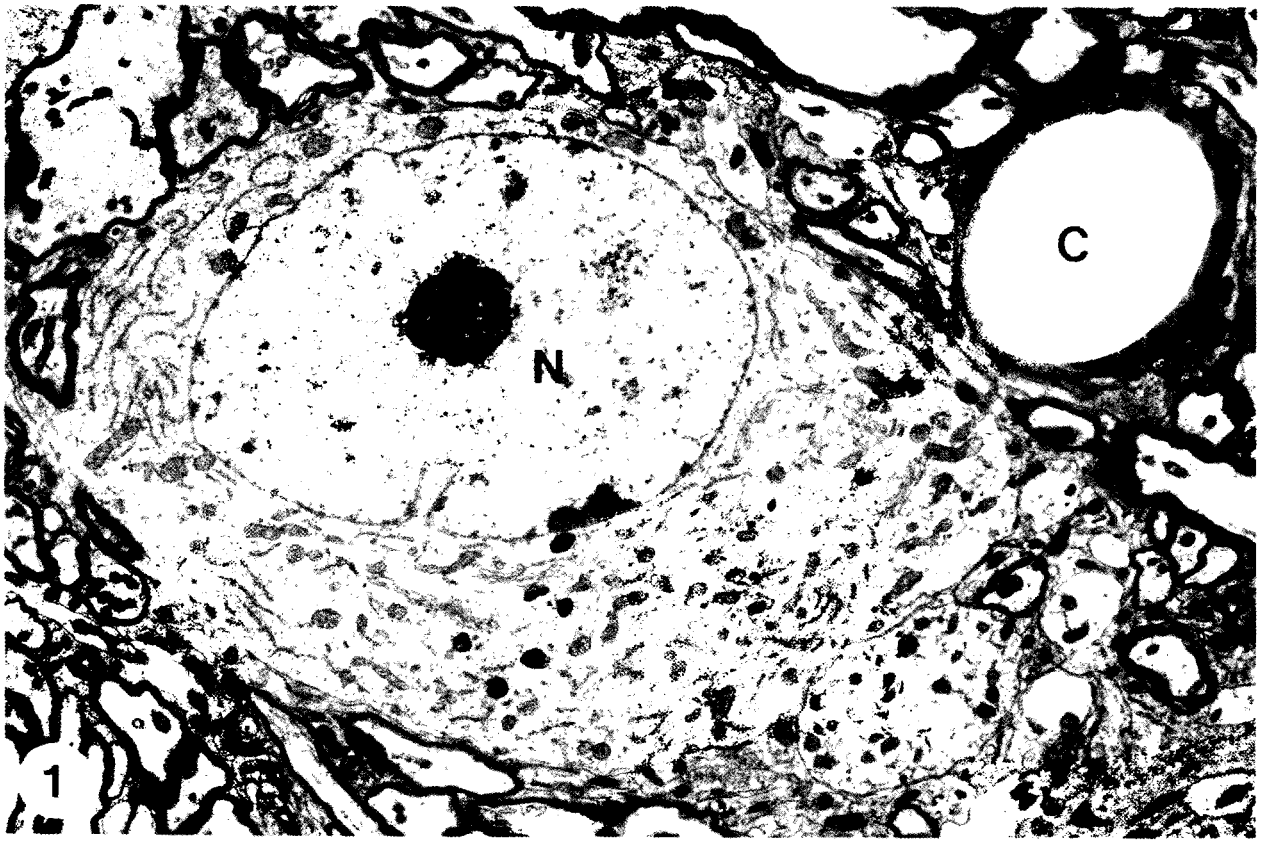

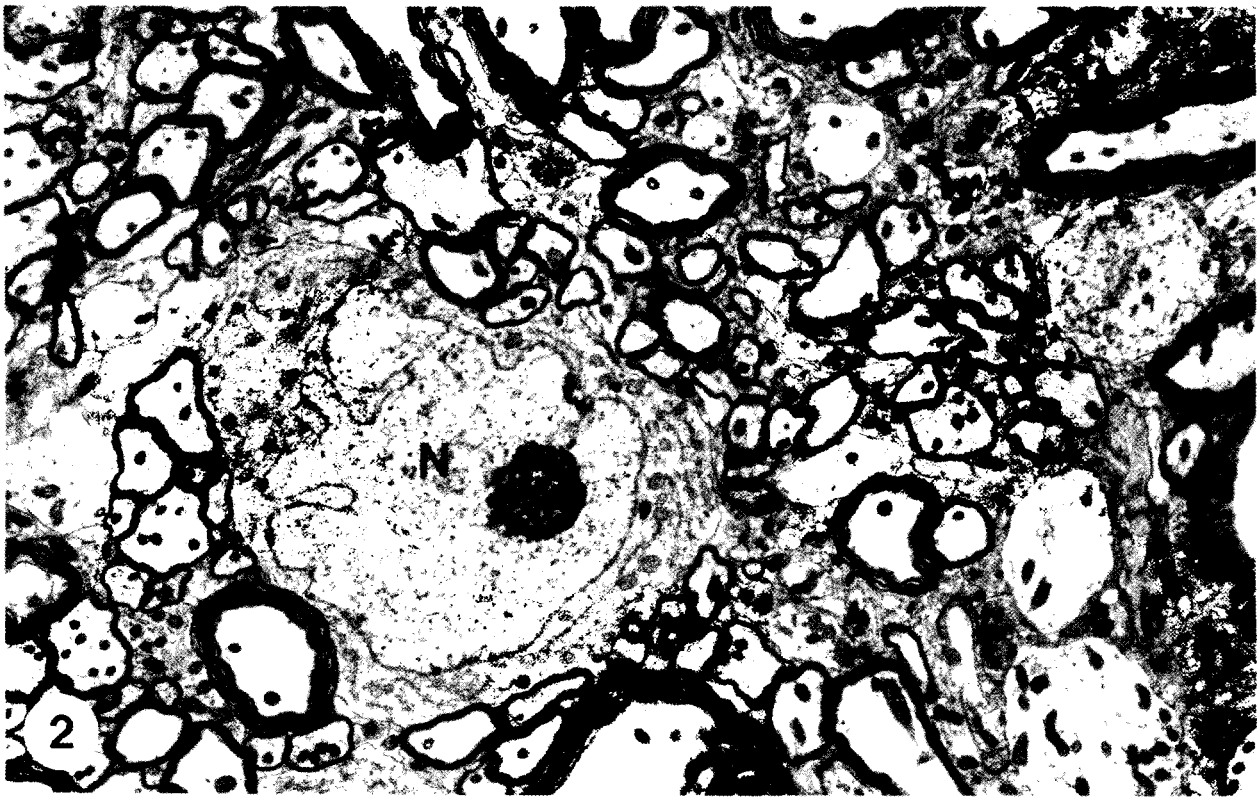


N
3


D
4


D1
D2
5

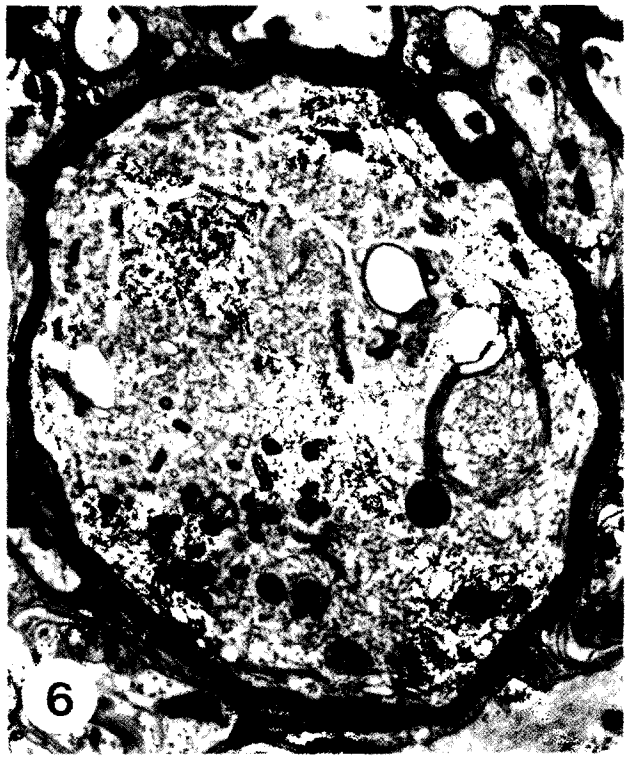
6


D
7


D
8


MA1
9

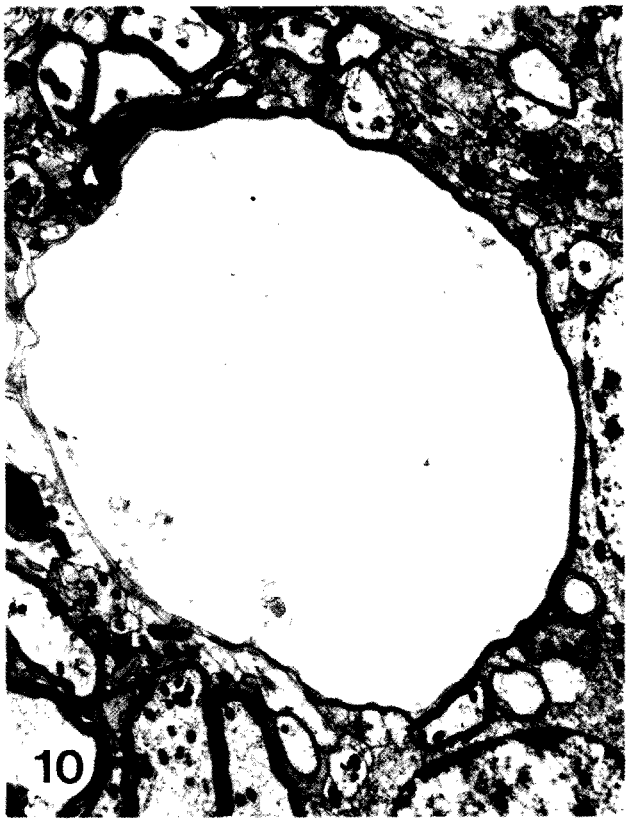
10

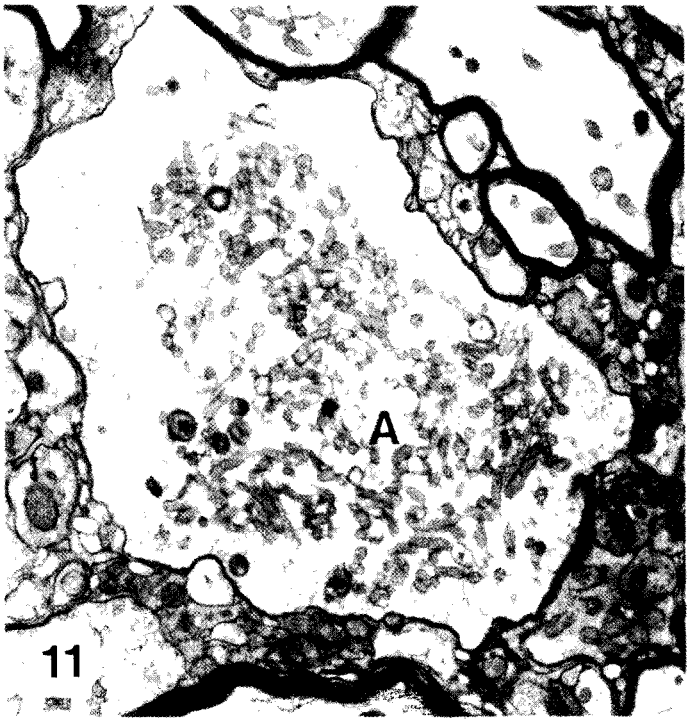

11

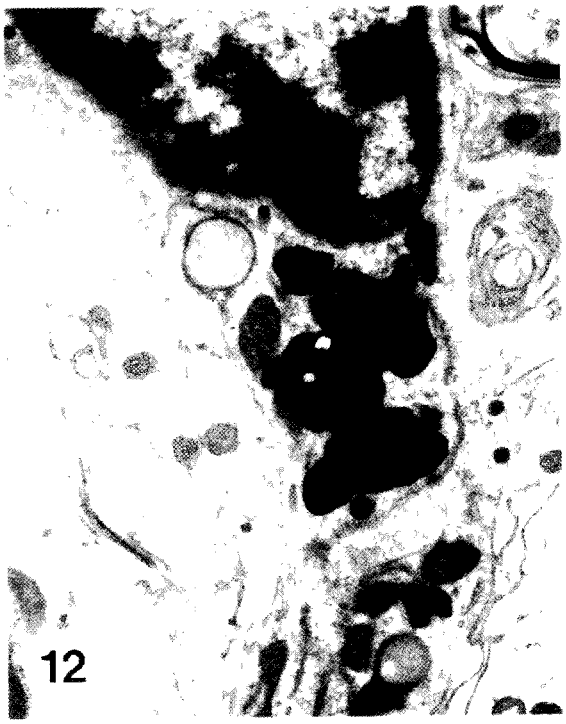

12

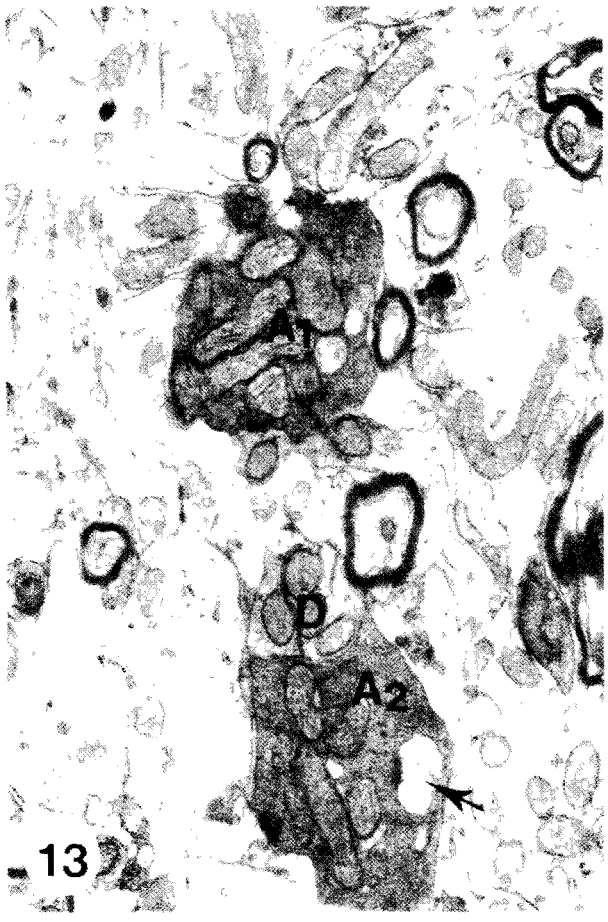

13

14


D1
A2
D2
15

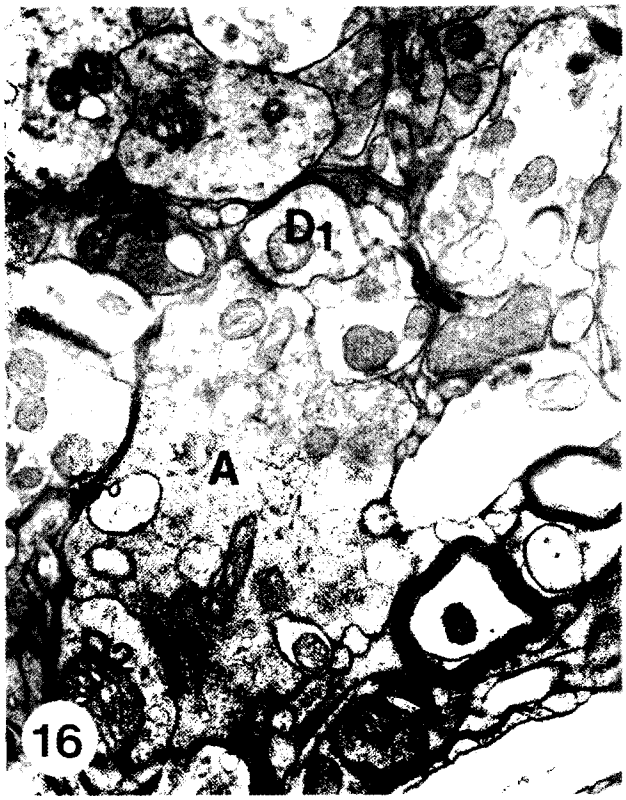
D1
A
16


17


18

Fig. 1. Electron micrograph of a medium-sized neuron from the gracile nucleus. Note the pale nucleus (N) with a smooth outline and the centrally placed nucleolus. In the neuropil there are numerous myelinated and unmyelinated axons, axon terminals, dendrites and a capillary (C). Control. × 6,000

Fig. 2. Electron micrograph of a small-sized neuron from the gracile nucleus. Note the large indented nucleus (N) with a thin rim of cytoplasm surrounding it. Observe the paucity of organelles, which include a Golgi apparatus, several cisternae of rough endoplasmic reticulum and a few mitochondria. Numerous myelinated axons are found in the neuropil. Control. × 6,000

Fig. 3. A large electron-dense axon terminal (A) showing swollen synaptic vesicles (arrows) and mitochondria. Note its close proximity to a neuronal cell body (N). 3 days post-diabetes. × 26,000

Fig. 4. A darkened axon terminal (A) containing highly swollen mitochondria (arrows) and synaptic vesicles. Note its close proximity to the dendrite (D). 3 days post-diabetes. × 20,000

Fig. 5. A swollen electron-dense axon terminal (A) appears to be presynaptic to two dendrites (D_1, D_2). Dendrites D_1 and D_2 show electron-lucent cytoplasm and mitochondria with swollen cristae. 3 days post-diabetes. × 25,000

Fig. 6. A large swollen and degenerating myelinated axon. Note the presence of vacuoles, glycogen particles, neurofilaments and tubulovesicular elements in its cytoplasm. 3 days post-diabetes. × 10,500

Fig. 7. A large darkened axon terminal (A_1) showing randomized small agranular vesicles and clustering of swollen mitochondria. Another axon terminal (A_2) is presynaptic to a dendrite (D). Note the clustering of mitochondria and small agranular vesicles (arrows). 7 days post-diabetes. × 17,500

Fig. 8. A large degenerating axon terminal (A) is presynaptic to a dendrite (D). Note the electron-dense cytoplasm, clustering of synaptic vesicles (arrows) and mitochondria. 7 days post-diabetes. × 17,500

Fig. 9. Two degenerating myelinated axons (MA_1, MA_2) in the gracile nucleus. MA_1 shows demyelination of the myelin sheath and an electron-lucent core. MA_2 also shows demyelination and detachment of the electron-dense core. 7 days post diabetes. × 10,500

Fig. 10. A large swollen electron-lucent myelinated axon undergoing degeneration. Note the amorphous axoplasm. Most of the other axonal profiles appear normal. 7 days post-diabetes. × 6,500

Fig. 11. A large swollen axon terminal (A) showing clustering of mitochondria and randomized synaptic vesicles. 1 month post-diabetes. × 10,500

Fig. 12. Electron micrograph showing a portion of a macrophage. The macrophage contains some highly digested electron-dense degenerating debris in its cytoplasm. Note the dense clumping of chromatin materials in its nucleus. 1 month post-diabetes. × 17,500

Fig. 13. Two freshly degenerating axon terminals (A_1, A_2) in the gracile nucleus. Axon terminal A_2 is in close apposition to an electron-dense dendrite (D). Note the presence of a dendritic excrescence (arrow) in the cytoplasm of the axon terminal (A_2). 3 months post-diabetes. × 17,500

Fig. 14. Electron micrograph of a process from a macrophage containing several degenerating electron-dense debris. 3 months post-diabetes. × 17,500

Fig. 15. Several degenerating axon terminals (A_1, A_2, A_3, A_4) showing electron-dense degeneration. Axon terminal A_1 is characterized by an electron-dense cytoplasm containing swollen mitochondria and synaptic vesicles. Axon terminals A_2 and A_3 appear to be presynaptic to dendrites D_1, D_2 respectively. 6 months post-diabetes. × 17,500

Fig. 16. A large degenerating axon terminal (A) is presynaptic to two dendrites (D_1, D_2). Note that most of the other profiles in the surroundings appear to be affected as well. 6 months post-diabetes. × 17,500

Fig. 17. Electron micrograph showing drastic demyelination of myelinated axons in the gracile nucleus. Note the numerous vacuoles (arrows) which are being formed in the myelin sheath. 6 months post-diabetes. × 11,500

Fig. 18. A degenerating unmyelinated axon showing accumulation of electron-dense glycogen particles at one pole. The adjacent neuronal profiles appear to be normal. 6 months post-diabetes. × 20,000

their cytoplasm (Fig. 12); presumably this debris was partially digested remains engulfed from the neuropil. Non-affected profiles appeared to be normal.

3 months post-diabetes

Freshly degenerating axon terminals were still present at this stage (Fig. 13). These degenerating axon terminals were mostly presynaptic to normal dendrites. A few degenerating dendrites were also observed in the neuropil of the gracile nucleus. Commonly seen scattered amongst the neuronal elements were the macrophages with their engulfed electron-dense debris (Fig. 14). Very often, these macrophages were found close to blood vessels. Several degenerating myelinated axons showing an electron-dense form of degeneration were also seen at this stage.

6 months post-diabetes

At 6 months post-diabetes, numerous degenerating axon terminals were still present. Each was characterized by an accumulation of small agranular synaptic vesicles and swollen mitochondria in an electron-dense cytoplasm. Some of these degenerating axon terminals made synaptic contacts with seemingly normal dendrites (Fig. 15). Adjacent to these degenerating axon terminals were numerous degenerating electron-dense dendrites (Fig. 16). Each affected dendrite was characterized by small traces of cisternae of endoplasmic reticulum and swollen mitochondria in an electron-dense cytoplasm. Several myelinated axons showing drastic degeneration were also encountered at this stage. Each degenerating myelinated axon was characterized by the detachment of the myelin sheath from the axonal core, thereby forming large vacuoles (Fig. 17). Most of the axonal cores of these degenerating profiles were electron dense. Some of the unmyelinated axons were also affected by the state of diabetes at this time interval. These unmyelinated axons usually showed vacuolations and accumulation of glycogen particles (Fig. 18) as well as neurofilaments. The neighbouring unaffected profiles in the neuropil appeared normal in their ultrastructure.

Discussion

The spontaneously diabetic BB rat is an established animal model for the study of diabetic neuropathy (Sima

and Thibert, 1982; Yagihashi and Sima, 1985a,b, 1986a,b). Recently, Sima and Yagihashi (1986) have shown ultrastructural changes in the central sensory nerve fibres of the gracile tract. The present study represents an extension of these observations to the gracile nucleus and has demonstrated the presence of neuropathy. The degenerative changes were observed as early as 3 days post-diabetes, and were clearly progressive, recurrent and possibly irreversible as displayed by their subsequent engulfment by macrophages. Darkened degenerating axon terminals were characterized by accumulation of small agranular vesicles and mitochondria in an electron-dense cytoplasm. Darkened dendrites contained swollen mitochondria and traces of cisternae of endoplasmic reticulum in an electron-dense cytoplasm. As these structural changes were rarely seen in the control animals, they have been attributed to the result of the condition of diabetes in the spontaneously diabetic BB rat. Both myelinated and unmyelinated axons also showed signs of degeneration. These degenerating profiles were identified by the presence of swollen mitochondria, vacuolations, accumulation of glycogen granules, tubulovesicular elements and dense lamellar bodies.

The pathogenesis of axonal dystrophy is still largely unknown. Dystrophic changes were originally described in preterminal axons of primary sensory neurons of the gracile and cuneate nuclei of vitamin E - deficient rats (Lampert et al., 1964). These changes were later documented in the same location in senile man and animals (Fujisawa and Shiraki, 1978; Schmidt et al., 1983). A recent study of axonopathy in the spontaneously diabetic BB rat has revealed an increased incidence of dystrophic changes in the gracile tract (Sima and Yagihashi, 1986). Several hypotheses have been proposed to explain the development of dystrophic changes (Jellinger, 1973). Intrinsic disturbances of axonal metabolism or reactions to chronic injury caused by diabetes mellitus at certain sites in the central nervous system may have resulted in the changes observed in the gracile nucleus of the spontaneously diabetic BB rat in the present study.

Proliferation of tubulovesicular elements has been widely accepted as the hallmark of dystrophic changes (Lampert et al., 1964; Lampert, 1967; Blakemore and Cavanagh, 1969; Jellinger, 1973; Schmidt et al., 1981). Tubulovesicular elements are also seen in normal aging (Jellinger, 1973; Fujisawa and Shiraki, 1978), in ligated axons (Griffin et al., 1977; Tsukita and Ishikawa, 1980), and a variety of toxic neuropathies such as those occurring after exposure to organophosphorus compounds (Bischoff, 1967, 1970; Prineas, 1969; Bouldin and Cavanagh, 1979), acrylamide (Suzuki and Pfaff, 1973; Schaumburg et al., 1974), and zinc pyridinethione (Sahenk and Mendell, 1979). In the present study, numerous degenerating axonal profiles in the gracile nucleus of the diabetic rats contained tubulovesicular elements. This tubulovesicular type of degeneration has also been described in the distal gracile tract as part of the diabetic central-peripheral polyneuropathy in the BB rat (Sima and Yagihashi, 1986). It is believed that the accumulation of tubulovesicular elements is derived from smooth endoplasmic reticulum being transported by the fast component of axoplasmic flow (Tsukita and Ishikawa, 1980). The fact that this type of degeneration is commonly seen in terminal axons or at sites where the axonal integrity is interrupted suggests a defect in the turnaround of materials transported by the fast anterograde transport (Jakobsen and Sidenius, 1979; Sidenius and Jakobsen, 1981).

Neuropathies exhibiting neurofilamentous abnormalities have been previously reviewed (Asbury and Brown, 1983; Griffin and Price, 1983). In the present study, in animals sacrificed after the onset of diabetes, neurofilamentous type of degeneration was consistently found in the axonal profiles. The mechanism responsible for the abnormal accumulation of neurofilaments in the central nervous system of the spontaneously diabetic BB rat is not known. It is believed that two factors may be of pathogenetic importance: 1) non-enzymatic glycation of cytoskeletal proteins (Williams et al., 1982); and 2) a defect in axoplasmic transport (Jakobsen and Sidenius, 1980; Mendell et al., 1981; Medori et al., 1985). It has been hypothesized that the hyperglycemic state results in increased glycation of structural proteins and subsequent inhibition of their proper assembly. The proper assembly of proteins may be further impaired by a decrease in polymerization of structural units due to a decrease in energy utilization mediated by an ATPase defect (Williams et al., 1982; Greene et al., 1984). Moreover, the impaired slow axoplasmic transport, as demonstrated in both streptozotocin-induced diabetic rat and spontaneously diabetic BB rat (Jakobsen and Sidenius, 1980; Medori et al., 1985), may lead to the proximal congestion of neurofilaments. Proximal accumulation of neurofilaments in both autonomic (sympathetic) and somatic nerves (Medori et al., 1985; Yagihashi and Sima, 1985a,b) of the BB rat has been shown to be accompanied by a progressive distal axonopathy (Sima et al., 1982, 1983; Sima, 1983).

It is hypothesized that some unknown trophic factors may be removed or reduced after the onset of diabetes, resulting in the dysmetabolism of the cell bodies, thereby affecting the axons, axon terminals and dendrites. In view of the recent discovery of insulin receptors in the central nervous system (Heidenreich et al., 1983; Clarke et al., 1984; Hendricks et al., 1984; Gammeloft et al., 1985; Lowe et al., 1986; Raizada et al., 1987), the onset of diabetes in the BB rat may have altered the configuration of the receptors present in the neuronal elements of the gracile nucleus. The nett effect is that the receptors may not be able to recognize and couple systematically with the insulin molecules circulated to the brain, thereby resulting in a dysfunction (probably via the metabolic pathway) in the neuronal elements. Further work at the receptor level using radioactive tracer or immunocytochemical techniques may bring to light the mechanism(s) involved in the changes observed in the gracile nucleus of the spontaneously diabetic BB rat.

Acknowledgements. The authors wish to thank Mr. T.Y. Yick of the EM Unit and Mr. A.A.J. Kamal for their technical assistance. They are grateful to Mrs. C. Wong for typing the manuscript.

This work was supported by Grant RP 870304 from the National University of Singapore

References

Asbury A.K. and Brown M.J. (1983). The evolution of structural changes in distal axonopathies. In: Experimental and clinical neurotoxicology. Spencer P.S. and Schaumburg H.H. (eds). Williams and Wilkins. Baltimore. pp 179-192.

Bischoff A. (1967). The ultrastructure of tri-ortho-cresyl phosphate poisoning. I. Studies on myelin and axonal alterations in the sciatic nerve. Acta Neuropathol. (Berl.) 9, 158-174.

Bischoff A. (1970). The ultrastructure of tri-ortho-cresyl phosphate poisoning in the chicken. II. Studies on spinal cord alterations. Acta Neuropathol. (Berl.) 15, 142-153.

Blakemore W.F. and Cavanagh J.B. (1969). «Neuroaxonal dystrophy» occurring in an experimental «dying back» process in the rat. Brain 92, 789-804.

Bouldin T.W. and Cavanagh J.B. (1979). Organophosphorus neuropathy: II. A fine-structural study of the early stages of axonal degeneration. Am. J. Pathol. 94, 253-270.

Clarke D.W., Boyd F.T. Jr., Kappy M.S. and Raizada M.K. (1984). Insulin binds to specific receptors and stimulates 2-deoxy-D-glucose uptake in cultured glial cells from rat brain. J. Biol. Chem. 259, 11672-11675.

Fujisawa K. and Shiraki H. (1978). Study of axonal dystrophy. I. Pathology of the neurophil of the gracile and cuneate nuclei in aging and old rats. A sterological study. Neuropathol. Appl. Neurobiol. 4, 1-20.

Gammeloft S., Fehlmann M. and Obberghen E. Van. (1985). Insulin receptors in the mammalian central nervous system: binding characteristics and subunit structure. Biochemie 67, 1147-1153.

Greene D.A., Yagihashi S., Lattimer S.A. and Sima A.A.F. (1984). Nerve Na^+–K^+–ATPase, conduction, and myo-inositol in the insulin-deficient BB rat. Am. J. Physiol. 247, E534-539.

Griffin J.W. and Price D.L. (1983). Proximal axonopathies induced by toxic chemicals. In: Experimental and clinical neurotoxicology. Spencer P.S. and Schaumburg H.H. (eds). Williams and Wilkins. Baltimore. pp 161-178.

Griffin J.W., Price D.L., Engel W.K. and Drachman D.B. (1977). The pathogenesis of reactive axonal swellings: Role of axonal transport. J. Neuropathol. Exp. Neurol. 36, 214-227.

Heidenreich, K.A., Zahniser N.R., Berhanu P., Brandenburg D. and Olefsky J.M. (1983). Structural differences between insulin receptors in the brain and peripheral target tissues. J. Biol. Chem. 258, 8527-8530.

Hendricks S.A., Agardh C.D., Taylor S.I. and Roth J. (1984). Unique features of the insulin receptor in rat brain. J. Neurochem. 43, 1302-1309.

Jakobsen J. and Sidenius P. (1979). Decreased axonal flux of retrogradely transported glycoproteins in early experimental diabetes. J. Neurochem. 30, 1055-1060.

Jakobsen J. and Sidenius P. (1980). Decreased axonal transport of structural proteins in streptozotocin diabetic rats. J. Clin. Invest. 66, 292-297.

Jellinger K. (1973). Neuroaxonal dystrophy: its natural history and related disorders. Prog. Neuropathol. 2, 129-180.

Lampert P.W. (1967). A comparative electron microscopic study of reactive, degenerating, regenerating and dystrophic axons. J. Neuropathol. Exp. Neurol. 26, 345-368.

Lampert P.W., Blumberg J.M. and Pentschew A. (1964). An electron microscopic study of dystrophic axons in the gracile and cuneate nuclei of Vitamin E - defficient rats. Axonal dystrophy in vitamin E defficiency. J. Neuropathol. Exp. Neurol. 23, 60-77.

Lowe W.J. Jr., Boyd F.T., Clarke D.W., Raizada M.K., Hart C. and LeRoith D. (1986). Development of brain insulin receptors: structural and functional studies of insulin receptors from whole brain and primary cell cultures. Endocrinology 119, 25-35.

Marliss E.B., Nakhooda A.F., Poussier P. and Sima A.A.F. (1982). The diabetic syndrome of the «BB» Wistar rat: possible relevance to type I (insulin-dependent) diabetes in man. Diabetologia 22, 225-232.

Medori R., Autilio-Gambetti L., Monaco S. and Gambetti P. (1985). Diabetic neuropathy: A new type of neurofilamentous axonopathy? J. Neuropathol. Exp. Neurol. 44, 345 (Abstract).

Mendell J.R., Sahenk Z., Warmolts J.R., Marshall J.K. and Thibert P. (1981). The spontaneously diabetic BB Wistar rat. Morphologic and physiologic studies of peripheral nerve. J. Neurol. Sci. 52, 103-115.

Nakhooda A.F., Like A.A., Chappel C.I., Murray F.T. and Marliss E.B. (1977). The spontaneously diabetic Wistar rat. Metabolic and morphologic studies. Diabetes 26, 100-112.

Nakhooda A.F., Like A.A., Chappel C.I., Wei C.N. and Marliss E.B. (1978). The spontaneously diabetic Wistar rat. Studies prior to and during development of the overt syndrome. Diabetologia 14, 199-207.

Prineas J.W. (1969). The pathogenesis of dying-back polyneuropathies. I. An ultrastructural study of experimental tri-ortho-cresyl phosphate intoxication in the cat. J. Neuropathol. Exp. Neurol. 28, 571-597.

Raizada M.K., Boyd F.T., Clarke D.W. and LeRoith D. (1987). Physiologically unique insulin receptors on neuronal cells. In: Insulin-like growth factors and their receptors in the central nervous system. Raizada M.K., Phillips M.I. and LeRoith D. (eds). Plenum Press. New York and London. pp 191-200.

Sahenk Z. and Mendell J.R. (1979). Ultrastructural study of zinc pyridenethione-induced peripheral neuropathy. J. Neuropathol. Exp. Neurol. 38, 532-550.

Schaumburg H.H., Wisniewski H.M. and Spencer P.S. (1974). Ultrastructural studies on the dying-back process. I. Peripheral nerve terminal in axon degeneration in systemic acrylamide intoxication. J. Neuropathol. Exp. Neurol. 33, 260-284.

Schmidt R.E., Nelson J.S. and Johnson E.M. Jr. (1981). Experimental diabetic autonomic neuropathy. Am. J. Pathol. 103, 210-225.

Schmidt R.E., Plurad S.B. and Modert C.W. (1983). Neuroaxonal dystrophy in the autonomic ganglia of aged rats. J. Neuropathol. Exp. Neurol. 42, 376-390.

Sidenius P. and Jakobsen J. (1981). Retrograde axonal transport. A possible role in the development of neuropathy. Diabetologia 20, 110-112.

Sima A.A.F. (1983). The development and structural

characterization of the neuropathies in the spontaneously diabetic BB-Wistar rat. Metabolism 32 (Suppl. 7) 106-111.

Sima A.A.F., Bouchier M. and Christensen H. (1983). Axonal atrophy in sensory nerve of the diabetic BB-Wistar rat: A possible early correlate of human diabetic neuropathy. Ann. Neurol. 13, 264-272.

Sima A.A.F., Lorusso A.C. and Thibert P. (1982). Distal symmetric polyneuropathy in the spontaneously diabetic BB-Wistar rat. An ultrastructural and teased fiber study. Acta Neuropathol. (Berl.) 58, 39-47.

Sima A.A.F. and Thibert P. (1982). Proximal motor neuropathy in the BB-Wistar rat. Diabetes 31, 784-788.

Sima A.A.F. and Yagihashi S. (1986). Central-peripheral distal axonopathy in the spontaneously diabetic BB-rat: ultrastructural and morphometric findings. Diabetes Res. Clin. Pract. 1, 289-298.

Suzuki K. and Pfaff L.D. (1973). Acrylamide neuropathy in rats. An electron microscopic study of degeneration and regeneration. Acta Neuropathol. (Berl.) 24, 197-213.

Tay S.S.W., Wong W.C. and Kamal A.A.J. (1988). The gracile nucleus in spontaneously diabetic BB-rats. Soc. Neurosc. (Abstract) 14, 338.

Tsukita S. and Ishikawa H. (1980). The movement of membranous organelles in axons. Electron microscopic identification of anterogradely and retrogradely transported organelles. J. Cell Biol. 84, 513-530.

Williams S.K., Howarth N.L., Devenny J.J. and Bitensky M.W. (1982). Structural and functional consequences of increased tubulin glycosylation in diabetes mellitus. Proc. Natl. Acad. Sci. USA 79, 6546-6550.

Yagihashi S. and Sima A.A.F. (1985a). Diabetic autonomic neuropathy in the BB rat. Ultrastructural and morphometric changes in sympathetic nerves. Diabetes 34, 558-564.

Yagihashi S. and Sima A.A.F. (1985b). Diabetic autonomic neuropathy. The distribution of structural changes in sympathetic nerves of the BB rat. Am. J. Pathol. 121, 138-147.

Yagihashi S. and Sima A.A.F. (1986a). Diabetic autonomic neuropathy in BB rat. Ultrastructural and morphometric changes in parasympathetic nerves. Diabetes 35, 733-743.

Yagihashi S. and Sima A.A.F. (1986b). Neuroaxonal and dendritic dystrophy in diabetic autonomic neuropathy. Classification and topographic distribution in the BB-rat. J. Neuropathol. Exp. Neurol. 45, 545-565.

Accepted July 16, 1990